

The Running of the Cosmological and the Newton Constant controlled by the Cosmological Event Horizon

Florian Bauer*

*Physik-Department, Technische Universität München,
James-Frank-Straße, D-85748 Garching, Germany*

26 January 2005

Abstract

We study the renormalisation group running of the cosmological and the Newton constant, where the renormalisation scale is given by the inverse of the radius of the cosmological event horizon. In this framework, we discuss the future evolution of the universe, where we find stable de Sitter solutions, but also “big crunch”-like and “big rip”-like events, depending on the choice of the parameters in the model.

1 Introduction

The recently observed [1] accelerated expansion of the universe may have its reason in the existence of dark energy (DE), an energy form with negative pressure, which is so far not understood. The cosmological constant (CC) is the theoretically simplest candidate for DE, because it occurs as a classical parameter in Einstein’s equations, and further it has an origin as vacuum energy in quantum field theory (QFT). On the other hand, it is difficult to explain the tiny value of the CC and the actual coincidence of the energy densities of the CC and non-relativistic matter [2].

There are lots of models, which describe DE as a dynamical quantity, e.g. by using scalar fields. Another possibility is the modification of the theory of gravity by introducing extra terms in the equations of the cosmological evolution, or extending our space-time by additional space-time dimensions. However, in most of these models the accelerated cosmic expansion is due to new and unknown physics, which often means a high amount of arbitrariness and limited predictability.

In this work, we investigate the CC in the sense that it emerges anyway on a formal level in QFT. There, the zero-point or vacuum energy of a quantised field has the same equation of state as the CC occurring in Einstein’s equations. Unfortunately, it is unknown how to calculate its value in a unique way, because it can be written in the form of a quartically divergent momentum integral like $\int d^3p \cdot p$. The naive assumption of an ultra-violet (UV) cutoff in this integral at some known energy scale usually leads to an unobserved high value of the CC, which is also called the old CC problem. However, the procedure of renormalisation of (coupling) constants in QFTs can handle infinities, thereby leading to a dependence of the renormalised constants on some energy scale μ . In many cases, this renormalisation scale can be identified with an external momentum, or at least with some characteristic scale (e.g. the temperature) of the environment. Studying QFT on curved space-time [3] leads to infinities in the vacuum expectation values (VEV) of the energy-momentum tensors of the fields. This can be treated by renormalisation to

*Email: fbauer@ph.tum.de

yield a scale-dependent or running CC and a running Newton constant (NC). The absolute values are still not calculable, but the change with respect to the renormalisation scale can be described by the renormalisation group equations (RGE). Unlike the running coupling constants in the standard model of particles, here, the physical meaning of the scale is not given by the theory. This becomes obvious since, in the language of Feynman graphs, the formally infinite value of the CC corresponds to a closed loop without external legs and hence no distinct energy scale. Connecting this renormalisation scale with physics thus requires an additional theoretical input. Usual choices in the literature are the Hubble scale, the square root of the Ricci scalar, and combinations of similar quantities. The RG running of the CC and the NC has been studied in several different frameworks and models, some recent results can be found in Refs. [4–8].

In our investigation of the RG running of the CC and the NC, we choose the inverse of the radius of the cosmological event horizon as the renormalisation scale. Such a horizon usually exists in accelerating universes like ours. In addition, the possible relevance of the horizon scale for DE has often been pointed out [9–11]. In section 2, we derive the RGEs and their dependence on the renormalisation scale and the parameters, mainly the field masses. Since the event horizon in an evolving universe is not constant in time, the CC and the NC are also time-dependent, implying that the usual covariant conservation equations for the energy momentum tensor have to be modified (section 3). In section 4, we discuss the properties of the new evolution equation for the cosmic scale factor and derive some conditions on the existence and the stability of the final states of the universe. The cosmic fate is the main point of the discussion, since the characteristic behaviour in the far future depends crucially on the parameters in the RGEs. In section 5, we illustrate the possible final states of the universe by showing some numerical solutions and their dependence on the parameters. Finally, section 6 contains our conclusions and some open points of this setup.

2 Renormalisation group equations

To formulate the RGEs for the CC and the NC G , we consider free quantum fields on a curved space-time, namely a Friedmann-Robertson-Walker (FRW) universe with a positive CC λ . For one fermionic and one bosonic degree of freedom with masses m_F and m_B , respectively, the 1-loop effective action can be written in the form [3]

$$S_{\text{eff}} = \int d^4x \sqrt{-g} \left[\frac{\text{Ric}}{16\pi G} - \Lambda + \left(D + \ln \frac{m_{F/B}}{\mu} \right) \cdot \left(\frac{m_F^4 - m_B^4}{32\pi^2} - \frac{\text{Ric}}{16\pi^2} \left[\left(\xi - \frac{1}{6} \right) m_B^2 - \frac{1}{12} m_F^2 \right] \right) \right] + C, \quad (1)$$

where $D = \frac{1}{2}\gamma_{\text{Euler}} + \lim_{n \rightarrow 4} (n-4)^{-1}$ is a divergent term, which does not depend on the renormalisation scale μ . Furthermore, ξ is a coupling constant¹, and the variable C represents all further terms in the effective action, that are neither proportional to the Ricci scalar Ric nor to the vacuum energy density $\Lambda := \lambda/(8\pi G)$.

The relevant β -functions in the $\overline{\text{MS}}$ -scheme for the vacuum energy density Λ and the NC G are obtained by the requirement that the effective action S_{eff} must not depend on the renormalisation scale μ ,

$$\mu \frac{dS_{\text{eff}}}{d\mu} = 0.$$

Because of this condition, Λ and G have to be treated as μ -dependent functions in Eq. (1), which have to obey the RGEs given by

$$\mu \frac{d\Lambda}{d\mu} = -\frac{m_F^4 - m_B^4}{32\pi^2}, \quad \mu \frac{d}{d\mu} \left(\frac{1}{G} \right) = -\frac{1}{\pi} \left[\left(\xi - \frac{1}{6} \right) m_B^2 - \frac{1}{12} m_F^2 \right].$$

Note, that the divergent term D has dropped out, leaving over just the masses $m_{F/B}$ and ξ . Assuming constant masses, the RGEs can be integrated. Hence, the equation for the vacuum energy density reads

$$\Lambda(\mu) = \Lambda_0 \left(1 - q_1 \ln \frac{\mu}{\mu_0} \right), \quad \Lambda_0 := \Lambda(\mu_0), \quad (2)$$

¹In the action $S = \int d^4x \sqrt{-g} \left[\frac{\text{Ric} - 2\lambda}{16\pi G} + \frac{1}{2} \phi_{;\alpha} \phi^{;\alpha} - \frac{1}{2} [m^2 + \xi \text{Ric}] \phi^2 \right]$ of a scalar field ϕ on a curved space-time, the constant ξ occurs in the coupling term $\xi \cdot \text{Ric} \cdot \phi^2$ between the scalar field and the Ricci scalar Ric .

where the sign of the parameter

$$q_1 := \frac{1}{32\pi^2\Lambda_0} (m_{\text{F}}^4 - m_{\text{B}}^4) \quad (3)$$

depends on whether bosons or fermions dominate. In this context, a real scalar field counts as one bosonic degree of freedom, and a Dirac field as four fermionic ones. The generalisation to more than one quantum field in the RGE, can be achieved by summing over the fourth powers of their masses. For the NC G we obtain the RGE in the integrated form

$$G(\mu) = \frac{G_0}{1 - q_2 \ln \frac{\mu}{\mu_0}}, \quad G_0 := G(\mu_0). \quad (4)$$

Again, we omit the generalisation to more fields, that follows from summing over the squared masses of the fields. For one bosonic and one fermionic degree of freedom the mass parameter q_2 is given by

$$q_2 := \frac{G_0}{\pi} \left[\left(\xi - \frac{1}{6} \right) m_{\text{B}}^2 - \frac{1}{12} m_{\text{F}}^2 \right]. \quad (5)$$

Finally, we remark, that Eq. (2) for the running vacuum energy density $\Lambda(\mu)$ was derived in a renormalisation scheme, which is usually associated with the high energy regime. Unfortunately, the corresponding covariantly derived equations for the low energy sector are not known yet [12]. Therefore, we prefer to work with the above RGEs, which were derived in a covariant way, and study the consequences and the constraints on the mass parameters q_1 and q_2 .

Next, we choose the renormalisation scale μ to be the inverse of the radius R of the cosmological event horizon. In the FRW universe the (radial) horizon radius R at the cosmic time t is given by

$$\mu^{-1} = R(t) := a(t) \cdot \int_t^\infty \frac{dt'}{a(t')}, \quad (6)$$

where $a(t)$ is the cosmic scale factor, corresponding to the line element²

$$ds^2 = dt^2 - a^2(t) \left(\frac{dr^2}{1 - kr^2} + r^2 d\Omega^2 \right).$$

For universes, which end within finite time, the upper limit of the integral in Eq. (6) should be replaced by the time when the universe ends.

The choice of the scale $\mu = R^{-1}$ can be motivated by the thermodynamical properties of the cosmological event horizon. This horizon emits radiation, whose temperature is given by the Gibbons-Hawking [13] temperature $T_{\text{GH}} = (2\pi R)^{-1}$, that is proportional to our renormalisation scale μ . For a comoving observer in a de Sitter universe the only cosmological energy scale is given by this temperature. We have to admit that this no prove of the rightness of this choice. On the other hand, the investigation of the cosmological evolution with this specific renormalisation scale is the main point of this work, and the resulting solutions are quite interesting. From Eq. (6) we see that in an evolving universe the event horizon radius R and thus the scale μ are usually not constant in time. Therefore, the vacuum energy density Λ and the NC G will be time-dependent, too. This requires a generalisation of the covariant conservation conditions, and complicates the solutions of Friedmann's equations.

3 Evolution equation for the scale factor

In this section, we derive the evolution equation for the cosmic scale factor $a(t)$ in the framework of the spatially isotropic and homogeneous FRW universe with a time-dependent CC and NC. On this background, radiation and pressureless matter (dust) can both be described by a perfect fluid with the energy density ρ and the pressure $p = \omega\rho$, where the constant ω characterises the equation of state³. The corresponding energy-momentum tensor for these energy forms reads

$$T^{\alpha\beta} = (\rho + p)u^\alpha u^\beta - pg^{\alpha\beta},$$

²The constant k fixes the spatial curvature of the universe.

³Dust: $\omega = 0$; radiation: $\omega = \frac{1}{3}$.

with u^α being the four-velocity vector field of the fluid. With our choice of the renormalisation scale, G and Λ depend only on the cosmic time t . From Einstein's equations

$$G^{\alpha\beta} = 8\pi G(\Lambda g^{\alpha\beta} + T^{\alpha\beta})$$

and from the contracted Bianchi identities $G^{\alpha\beta}{}_{;\beta} = 0$ for the Einstein tensor $G^{\alpha\beta}$, we obtain the generalised conservation equations⁴

$$0 = [G\Lambda g^{\alpha\beta} + GT^{\alpha\beta}]_{;\beta} \stackrel{\alpha=0}{=} \dot{G}(\Lambda + \rho) + G(\dot{\Lambda} + \dot{\rho} + 3\frac{\dot{a}}{a}\rho(1 + \omega)).$$

Note that the simple scaling rule $\rho \propto a^{-3(1+\omega)}$ for the matter content is not valid anymore, because it is now possible to transfer energy between the matter and the vacuum, in addition to $\dot{G} \neq 0$. Therefore, we have to combine the Friedmann equations for the Hubble scale $H := \frac{\dot{a}}{a}$ and the acceleration $\frac{\ddot{a}}{a}$,

$$\left(\frac{\dot{a}}{a}\right)^2 + \frac{k}{a^2} = \frac{8\pi}{3}G(t)(\Lambda(t) + \rho(t)), \quad (7)$$

$$\frac{\ddot{a}}{a} = \frac{8\pi}{3}G(t)(\Lambda(t) - Q\rho(t)), \quad Q := \frac{1}{2}(1 + 3\omega), \quad (8)$$

to eliminate the matter energy density ρ . The left-hand side of the result is abbreviated by $F(t)$:

$$F(t) := \frac{\ddot{a}}{a} + Q \left[\left(\frac{\dot{a}}{a}\right)^2 + \frac{k}{a^2} \right] = \frac{8\pi}{3}G\Lambda \cdot (1 + Q). \quad (9)$$

Now the RGEs for Λ and G from Eqs. (2) and (4) are inserted in Eq. (9) to yield, with the specific choice of our renormalisation scale $\mu = 1/R$, the main equation of this work:

$$\frac{\mu_0}{\mu(t)} = \frac{R(t)}{R_0} = \exp \left[\frac{K_0 F(t) - 1}{q_1 - q_2 K_0 F(t)} \right]. \quad (10)$$

In this equation the constant K_0 is defined as

$$K_0 := \frac{3}{8\pi G_0 \Lambda_0 (Q + 1)} = \frac{H_0^{-2}}{\Omega_{\Lambda 0} (Q + 1)}, \quad (11)$$

where $\Omega_{\Lambda 0} = 8\pi G_0 \Lambda_0 / (3H_0^2)$ is the relative vacuum energy density and H_0 the Hubble scale at the time $t = t_0$.

Note that for a dominant matter energy density $\rho \gg \Lambda$ and flat spatial curvature ($k = 0$), the acceleration quantity $q := \frac{\ddot{a}}{a^2}$ is given by the negative value of the (new) equation of state parameter $Q = (1 + 3\omega)/2$, which we have introduced in Eq. (8).

4 Discussion

This section is devoted to the discussion of the properties of our main equation (10), thereby placing special interest in the late-time behaviour of the scale factor $a(t)$. Solving Eq. (10) for F leads to

$$K_0 F = \frac{1 + q_1 \ln \frac{R}{R_0}}{1 + q_2 \ln \frac{R}{R_0}}, \quad (12)$$

which is plotted as a function of the horizon radius R in Figs. 4, 5, 6 and 7 for four cases, depending on the signs of q_1 and q_2 . For reasonable field masses m , the magnitude of the mass parameter q_1 is always greater than that of q_2 . In the definition of the parameter q_2 the field masses m are divided by today's Planck mass $M_{\text{Planck},0} = 1/\sqrt{G_0}$, therefore, $|q_2|$ is a tiny quantity today. This implies a very weak running of the NC G , which agrees with the strong bounds on the time-variation of G [14]. Additionally, this has the advantage, that today we are far away from the Landau pole of $G(\mu)$, where the function F

⁴We do not assume $T^{\alpha\beta}{}_{;\beta} = 0$.

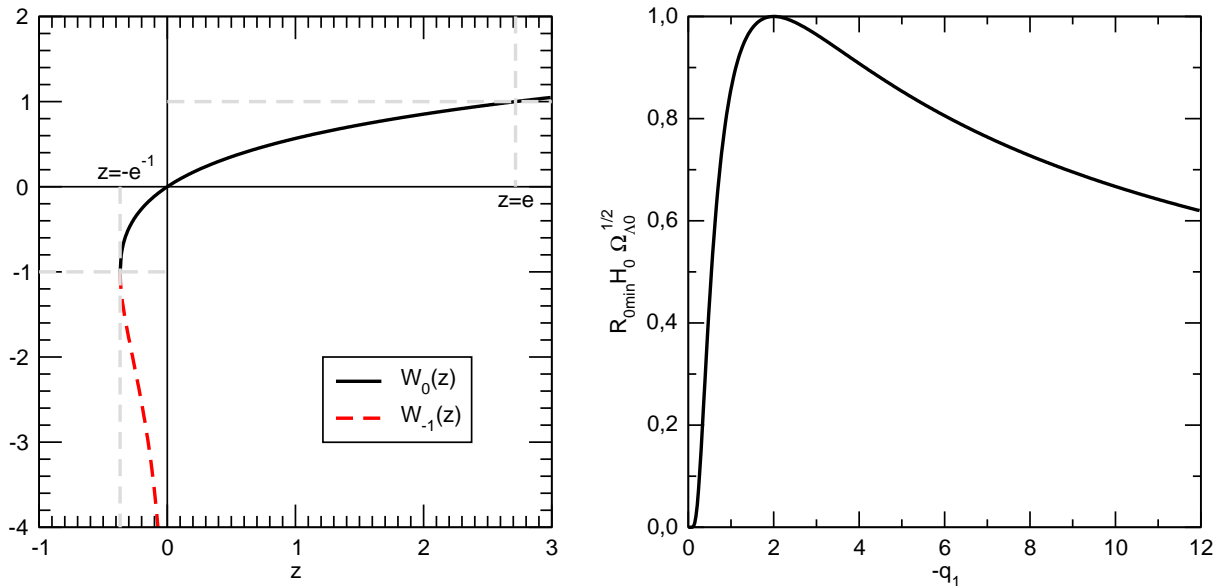


Figure 1: Left: The real-valued branches of Lambert's W -function $W_u(z)$, $u = 0, -1$. Right: The lower bound $R_{0\min}$ of the initial event horizon radius R_0 for negative q_1 . For $R_0 < R_{0\min}$ a final de Sitter state does not exist.

diverges. Very high values of $|F|$ could render our calculations invalid, since we do not implement higher powers of the curvature scalar in the gravitational action. These contributions are probably relevant in regimes with large $|F|$. Whether they are able to prevent the singular behaviour in the scale factor, that occurs in the numerical solutions for some cases, requires further investigation and is not treated in this paper.

Much less problematic are final states of the universe, that are de Sitter-like. In this case, the scale factor acquires the form $a(t) \propto \exp(H_e t)$ for large t , where H_e denotes the constant Hubble scale, and the radius of the event horizon is given by $R_e = 1/H_e$. Plugging this asymptotic form for $a(t)$ in Eq. (12), one arrives at

$$\frac{K_0(1+Q)}{R_e^2} = q_3 x^{-2} = \frac{1+q_1 \ln x}{1+q_2 \ln x},$$

where the variables $x := R_e/R_0$ and $q_3 := K_0(1+Q)/R_0^2 > 0$ have been introduced. Neglecting the running of the NC, we set $q_2 = 0$ and therefore we have to solve $q_3 x^{-2} = 1+q_1 \ln x$ for x . The results are given by

$$x = \frac{R_e}{R_0} = \sqrt{\frac{2q_3}{q_1 \cdot W_u\left(\frac{2q_3}{q_1} e^{2/q_1}\right)}}, \quad (13)$$

involving Lambert's W -function $W_u(z)$, which is the inverse function of $z = xe^x$. The index u denotes the different branches of this function. Only for $u = 0, -1$ it takes on real values for real arguments $z > -e^{-1}$. Additionally, $W_{-1}(z)$ is not real-valued for $z \geq 0$, as can be seen in Fig. 1, where both branches are plotted. From these properties of the W -function we get for negative q_1 the constraint $q_3 \leq -\frac{q_1}{2} \exp(-\frac{2}{q_1} - 1)$, which implies an lower bound for the initial value R_0 of the horizon radius:

$$R_0 \geq R_{0\min} := \sqrt{-\frac{2}{q_1 \Omega_{\Lambda 0} H_0^2} \exp\left(\frac{2}{q_1} + 1\right)}.$$

If R_0 is smaller than this minimal value, then Eq. (13) has no positive solutions and a final de Sitter state does not exist. For $R_0 = R_{0\min}$ there is exactly one solution $x = \exp(-\frac{1}{q_1} - \frac{1}{2})$, for higher values R_0 there are two solutions. In the case of a positive value of the parameter q_1 , the initial value R_0 must be smaller than $1/\sqrt{H_0^2 \Omega_{\Lambda 0}}$. Otherwise the final horizon radius R_e is smaller than the initial one, $x < 1$. Both cases are plotted in Fig. 2.

Since we have found several de Sitter solutions, we have to study the stability of these final states.

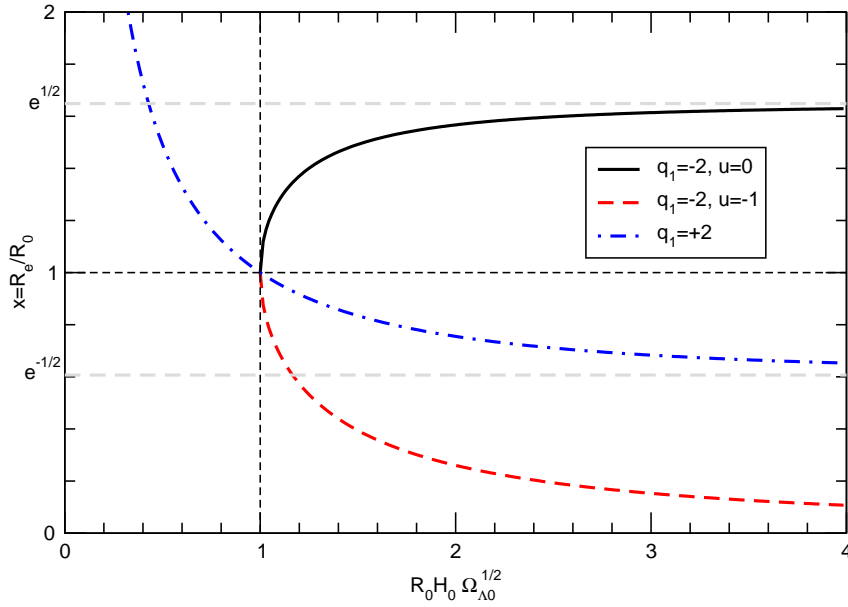


Figure 2: The ratio x between the final event horizon radius R_e and the initial radius R_0 as a function of R_0 , Eq. (13). Here q_1 is set to ± 2 and $q_2 = 0$. All stable de Sitter final states lie on the curve $q_2 = -2$, $u = 0$.

Therefore, we write $K_0\dot{F}$ as a function of $K_0F = K_0(\dot{H} + (Q+1)H^2)$,

$$K_0\dot{F} = q_1 \left[H - \frac{1}{R_0} \exp\left(\frac{1 - K_0F}{q_1}\right) \right],$$

where we used $\dot{R} = RH - 1$. In the final de Sitter state we have $K_0\dot{F} = 0$ and $R = R_e = 1/H_e = \text{const.}$ Near this point we can neglect \dot{H} in the function F and replace H by $\sqrt{\frac{K_0F}{K_0(Q+1)}}$. For a stable solution it is required that

$$\frac{d(K_0\dot{F})}{d(K_0F)} < 0$$

in the final point, where $K_0F = K_0(Q+1)H_e^2 = q_3x^{-2}$. With q_3 and x from above, this yields the stability condition

$$\left[W_u\left(\frac{2q_3}{q_1} e^{2/q_1}\right) \right]^{-1} < -1,$$

implying that there are no stable de Sitter solutions for positive values of q_1 , because the W -function is positive. For negative q_1 we get the condition

$$W_u\left(\frac{2q_3}{q_1} e^{2/q_1}\right) > -1,$$

which means that only the solution with $u = 0$ is stable. This renders the final event horizon radius $R_e = R_0x$ unique.

Finally, we take a closer look at the ratio R_e/R_0 as a function of the mass parameter q_1 . For initial values $R_0 < 1/(H_0\sqrt{\Omega_{\Lambda 0}})$, which means $q_3 > 1$, there is a certain range of values of q_1 where no solutions for R_e exist. This range is again given by the requirement that the argument of the W -function must be greater than or equal to $-e^{-1}$, leading to the conditions

$$q_1 \leq \frac{2}{W_0\left(-\frac{1}{eq_3}\right)} \quad \text{or} \quad q_1 \geq \frac{2}{W_{-1}\left(-\frac{1}{eq_3}\right)}. \quad (14)$$

In Fig. 3 the exclusion range for q_1 is obvious for $q_3 > 1$. In the case that q_1 lies above this range, the unstable solution for R_e is reached first during the future cosmic evolution. For q_1 below this range, the stable solution is nearer to the initial value R_0 than the unstable one, however, both solutions for R_e lie below R_0 . Initial values $R_0 > 1/(H_0\sqrt{\Omega_{\Lambda 0}})$ (i.e. $q_3 < 1$) lead to stable final states with $R_e > R_0$ for all negative values of q_1 .

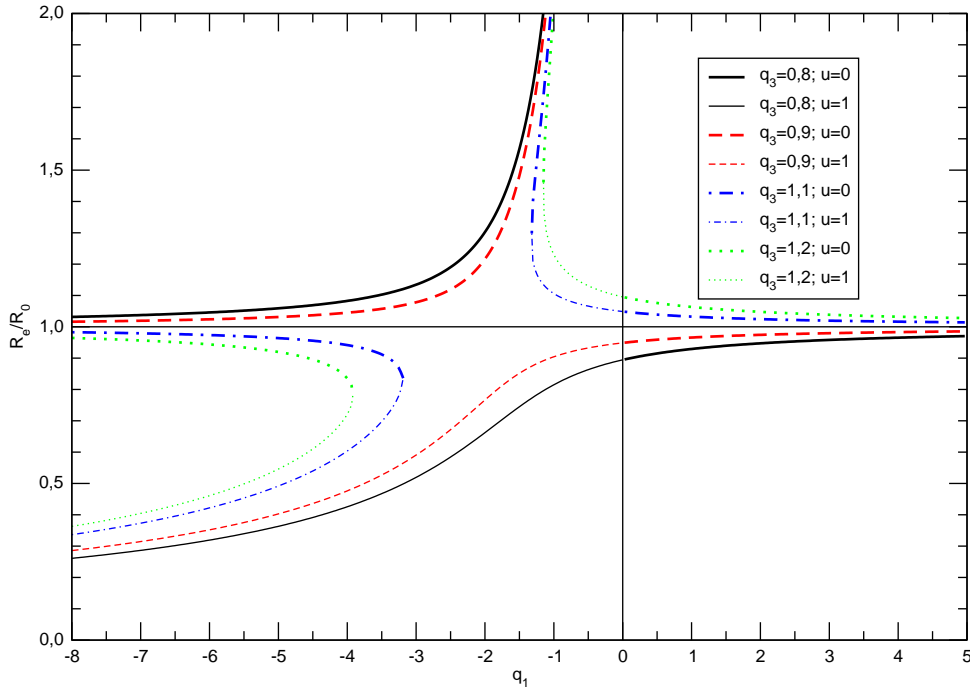


Figure 3: This figure shows the ratio R_e/R_0 between the final and the initial event horizon radius as a function of q_1 . We plotted four cases for different values of $q_3 = 1/(H_0^2 R_0^2 \Omega_{\Lambda 0})$, where the choice $q_3 = 0, 8; 0, 9$ corresponds to an initial radius $R_0 > 1/(H_0 \sqrt{\Omega_{\Lambda 0}})$, and $q_3 = 1, 1; 1, 2$ to $R_0 < 1/(H_0 \sqrt{\Omega_{\Lambda 0}})$. In the latter case there are no solutions for a certain range of values of q_1 as described by Eq. (14). The thick lines show the ($u = 0$)-branch of R_e/R_0 , and the thin lines the ($u = -1$)-branch, respectively.

For initial values R_0 and mass parameters q_1 , that do not satisfy the above existence and stability conditions, the fate of the universe will be “big crunch”-like or “big rip”-like⁵, respectively. With these notations we mean that the scale factor $a(t)$ or one of its derivatives H, q becomes singular in a finite time in the future. There is one exception, that may occur when q_1 and q_2 are both positive, where the function F and thus the Hubble scale H approach constant values, while the horizon radius R goes to infinity, see Fig. 7. Another property of the cosmic evolution for negative q_1 is that no big crunch may occur. This can be seen from the time-derivative of the function $K_0 F$,

$$K_0 \dot{F} = q_1 \frac{\dot{R}}{R} = q_1 \left(H - \frac{1}{R} \right), \quad q_1 < 0,$$

which gets positive for $H < 0$ (big crunch), thus preventing a further decrease of $K_0 F$ and the final collapse of the scale factor.

5 Numerical solutions

Up to this section, we analysed the evolution equation (10) for the scale factor analytically. Unfortunately, finding explicit solutions seems to be rather difficult because of the strongly non-linear form of the equation. Therefore, we solve it numerically, thereby realising that the form given by Eq. (10) is not directly suitable for a numerical study because of the integral over the time t in the radius function $R(t)$. This integral can be removed by differentiating with respect to t , leading to an ordinary differential equation of the order three,

$$\left[\frac{\dot{a}}{a} + \frac{(q_2 - q_1) K_0 \dot{F}}{(q_1 - q_2 K_0 F)^2} \right] \cdot \exp \left[\frac{K_0 F - 1}{q_1 - q_2 K_0 F} \right] - \frac{1}{R_0} = 0,$$

⁵Recent analyses of future singularities and their properties can be found in Refs. [15].

which can be solved for the scale factor $a(t)$ numerically. Note that one has to check whether the numerical solutions are also solutions of the original equation. This is not guaranteed since differentiating Eq. (10) possibly changes its set of solutions. Indeed, we encounter such “false” solutions in some cases.

Regarding recent observations, we get acceptable solutions only for $|q_1|$ to be of the order 1, which means that the relevant mass scale m should be near $\Lambda_0^{1/4} \sim 10^{-3}$ eV. Actually, the only known particles with such a low mass are neutrinos. This indicates that the influence of higher mass fields is suppressed, or these fields have decoupled, respectively. Unfortunately, the simple form of the RGEs (2) and (4) cannot account for a decoupling mechanism. Therefore, we assume in this work that the mass scale m is low enough today, so that the solutions are compatible with observations. However, note that at earlier cosmic times high-mass fields m should be relevant.

Concerning the differential equation, we can fix several initial conditions by using observational results. These are today’s value of the Hubble scale $H_0 = \frac{\dot{a}}{a}(t_0)$ and the relative vacuum energy density $\Omega_{\Lambda 0}$. Neglecting the spatial curvature ($\Omega_{k0} = -k/\dot{a}^2 = 0$) and considering only dust (with an equation of state parameter $Q = 0,5$) and the CC as relevant energy forms in the present-day universe, the acceleration parameter $q_0 = \frac{\ddot{a}a}{\dot{a}^2}(t_0)$ is determined by Eq. (9): $q = \Omega_{\Lambda}(1 + Q) + Q(\Omega_k - 1)$. Today’s value of the horizon radius R_0 is unknown, so we have to estimate it. Since it should be the largest physical length scale and the universe seems to be almost de Sitter-like, we assume the horizon radius to be around $R_0 \approx 1,2 \cdot H_0^{-1}$.

For the numerical treatment every dimensionful quantity is expressed in terms of today’s Hubble scale H_0 (Hubble units). In a Λ CDM universe with constant Λ and G , the cosmic age is denoted by t_0 . In our calculations we used the following numbers from Ref. [16]:

$$H_0 = 1,5 \cdot 10^{-42} \text{ GeV}, \quad \Omega_{\Lambda 0} = 0,73, \quad t_0 = 13,7 \text{ Gyr} = 0,99 \cdot H_0^{-1},$$

$$\Lambda_0 = 2,98 \cdot 10^{-47} \text{ GeV}^4, \quad \Lambda_0^{1/4} \approx 2,34 \cdot 10^{-3} \text{ eV}, \quad G_0 = (1,22 \cdot 10^{19} \text{ GeV})^{-2}.$$

The first observation from the numerical solutions is, that for a positive value of q_1 the cosmic age decreases with respect to the age t_0 of the standard Λ CDM universe, whereas for a negative q_1 the age increases. Furthermore, the usually small value of q_2 leads to a negligible time variation of Newton’s constant $G(t)$.

To show the characteristic future cosmic evolution, we investigate four cases in more detail, which result from the parameter choices $q_1 = \pm 2$ and $q_2 = \pm 0,1$. Note that due to the suppression by the Planck scale, the realistic value of q_2 should be much lower than $\pm 0,1$. Here, we used a large value for q_2 to show the differences due to the sign of q_2 . Figures 4–7 show the numerical results for different values of the initial radius R_0 of the event horizon. The graphs in each of the four figures illustrate the scale factor $a(t)$, the Hubble scale $H(t)$, the acceleration $q(t)$, the event horizon radius $R(t)$, and $F(t)$ as functions of the cosmic time t , respectively. The last graph displays $K_0 F$ as a function of the radius R/R_0 .

In section 4 we discussed the evolution equation analytically, and we found several conditions for the existence of stable de Sitter final states. These properties are also shown by the numerical results. For negative values of q_1 , we observe only “big rip”-like solutions and de Sitter final states, whereas for positive q_1 , a big crunch may also occur, and all de Sitter states are unstable. Note that the catastrophic events, the “big rip” and the “big crunch”, usually involve a high gravitational strength, implying that our calculations may not be reliable near these singular points. For positive values of q_1 and q_2 (see Fig. 7), we have not observed any “big rip”-like solutions. Then the final state may be either a “big crunch” or a forever expanding universe, where the Hubble scale approaches a finite positive value, but the event horizon radius R goes to infinity. This is a contradiction, because an asymptotically constant Hubble scale $H > 0$ implies a finite event horizon radius $R \approx H^{-1}$ in the far future, which is not the case here. Obviously, this numerical solution is not a solution of the original equation (10). For $q_1 > 0$ and $q_2 < 0$ (see Fig. 6) the “big rip”-like events in the numerical solutions occur at a finite and large value of the horizon radius R . Again, this behaviour is not compatible with the vanishing of the horizon radius at such an event. Therefore, we can reject these numerical solutions, too.

6 Conclusions

We investigated a cosmological model, where the CC and the NC are determined by renormalisation group equations, which emerge from QFT on curved space-time. By choosing the inverse radius of the

cosmological event horizon as the renormalisation scale, we get time-dependent constants. Because of this, the evolution equation for the cosmic scale factor becomes more complicated than in standard Λ CDM-cosmology, leading to cosmological solutions with several very different future final states of the universe. We found “big crunch”-like and “big rip”-like solutions, but also stable de Sitter final states. Which of these states will be realised depends crucially on the field masses in the renormalisation group equations, and on the initial value of today’s radius of the event horizon. In this context, we derived some conditions on the existence of stable de Sitter states. Furthermore, the cosmic evolution was analysed numerically for different values of the field masses. For a realistic cosmic behaviour, we have to require that the masses in the RGEs should be quite low, implying the need for some suppression or decoupling mechanism for high-mass fields. However, such a mechanism for the CC and the NC has not been found yet [12]. This also restricts the main focus of this work to the future behaviour of the universe, because for the cosmic evolution at early times quantum fields with high masses should be taken into account. Moreover, the regimes with a high gravitational strength need a deeper investigation, because such conditions are given not only at early times, but also at the singularities in the future. Finally, we conclude, that the specific choice of the renormalisation scale in this work leads to cosmological solutions, that may become singular in a finite time without introducing exotic forms of matter.

Acknowledgements

I would like to thank M. Lindner for useful comments and discussions. This work was supported by the “Sonderforschungsbereich 375 für Astroteilchenphysik der Deutschen Forschungsgemeinschaft”, and I wish to thank the Freistaat Bayern for a “Promotionsstipendium”.

References

- [1] A.G. Riess *et al.* [Supernova Search Team Collaboration], *Astron. J.* 116 (1998) 1009, [astro-ph/9805201](#); S. Perlmutter *et al.* [Supernova Cosmology Project Collaboration], *Astrophys. J.* 517 (1999) 565, [astro-ph/9812133](#).
- [2] S. Weinberg, *Rev. Mod. Phys.* 61 (1989) 1.
- [3] N.D. Birrell, P.C.W. Davies, “Quantum Fields in Curved Space”, Cambridge, Uk: Univ. Pr. (1982).
- [4] I.L. Shapiro, J. Sola, *Phys. Lett. B* 475 (2000) 236, [hep-ph/9910462](#); I.L. Shapiro, J. Sola, C. Espana-Bonet, P. Ruiz-Lapuente, *Phys. Lett. B* 574 (2003) 149, [astro-ph/0303306](#); I.L. Shapiro, J. Sola, [hep-ph/0305279](#); I.L. Shapiro, J. Sola, [astro-ph/0401015](#); I.L. Shapiro, J. Sola, H. Stefancic, [hep-ph/0410095](#).
- [5] A. Babic, B. Guberina, R. Horvat, H. Stefancic, *Phys. Rev. D* 65 (2002) 085002, [hep-ph/0111207](#); B. Guberina, R. Horvat, H. Stefancic, *Phys. Rev. D* 67 (2003) 083001, [hep-ph/0211184](#); A. Babic, B. Guberina, R. Horvat, H. Stefancic, [astro-ph/0407572](#).
- [6] M. Reuter, C. Wetterich, *Phys. Lett. B* 188 (1987) 38; M. Reuter, *Phys. Rev. D* 57 (1998) 971, [hep-th/9605030](#); M. Reuter, [hep-th/0012069](#); D.F. Litim, *Phys. Rev. D* 64 (2001) 105007 [hep-th/0103195](#); A. Bonanno, M. Reuter, *Phys. Rev. D* 65 (2002) 043508, [hep-th/0106133](#); A. Bonanno, M. Reuter, *Phys. Lett. B* 527 (2002) 9, [astro-ph/0106468](#); O. Lauscher, M. Reuter, *Phys. Rev. D* 65 (2002) 025013, [hep-th/0108040](#); O. Lauscher, M. Reuter, *Class. Quant. Grav.* 19 (2002) 483, [hep-th/0110021](#); O. Lauscher, M. Reuter, *Int. J. Mod. Phys. A* 17 (2002) 993, [hep-th/0112089](#); A. Bonanno, M. Reuter, *Int. J. Mod. Phys. D* 13 (2004) 107, [astro-ph/0210472](#); E. Bentivegna, A. Bonanno, M. Reuter, *JCAP* 0401 (2004) 001, [astro-ph/0303150](#); A. Bonanno, G. Esposito, C. Rubano, *Gen. Rel. Grav.* 35 (2003) 1899, [hep-th/0303154](#); M. Reuter, H. Weyer, [hep-th/0311196](#); D.F. Litim, *Phys. Rev. Lett.* 92 (2004) 201301, [hep-th/0312114](#); A. Bonanno, G. Esposito, C. Rubano, [gr-qc/0403115](#); M. Reuter, H. Weyer, *JCAP* 0412 (2004) 001, [hep-th/0410119](#); M. Reuter, H. Weyer, *Phys. Rev. D* 70 (2004) 124028, [hep-th/0410117](#); A. Bonanno, M. Reuter, [hep-th/0410191](#); J.W. Moffat, [astro-ph/0412195](#).

- [7] O. Bertolami, J.M. Mourao, J. Perez-Mercader, Phys. Lett. B 311 (1993) 27; E. Elizalde, S.D. Odintsov, I.L. Shapiro, Class. Quant. Grav. 11 (1994) 1607, [hep-th/9404064](#); O. Bertolami, J. Garcia-Bellido, Int. J. Mod. Phys. D 5 (1996) 363, [astro-ph/9502010](#); E. Elizalde, C.O. Lousto, S.D. Odintsov, A. Romeo, Phys. Rev. D 52 (1995) 2202, [hep-th/9504014](#); S. Falkenberg, S.D. Odintsov, Int. J. Mod. Phys. A 13 (1998) 607, [hep-th/9612019](#); L.N. Granda, S.D. Odintsov, Grav. Cosmol. 4 (1998) 85, [gr-qc/9801026](#); E. Verlinde, H. Verlinde, JHEP 0005 (2000) 034, [hep-th/9912018](#); J.A. Belinchon, T. Harko, M.K. Mak, Class. Quant. Grav. 19 (2002) 3003, [gr-qc/0108074](#).
- [8] I.L. Shapiro, J. Sola, JHEP 0202 (2002) 006, [hep-th/0012227](#); C. Espana-Bonet, P. Ruiz-Lapuente, I.L. Shapiro, J. Sola, JCAP 0402 (2004) 006, [hep-ph/0311171](#).
- [9] S. Thomas, [hep-th/0010145](#); S.D.H. Hsu, [hep-th/0403052](#); M. Li, [hep-th/0403127](#); Q.G. Huang, Y.G. Gong, [astro-ph/0403590](#); Y. Gong, [hep-th/0404030](#); R. Horvat, [astro-ph/0404204](#); Q.G. Huang, M. Li, [astro-ph/0404229](#); S. Carneiro, J.A.S. Lima, [gr-qc/0405141](#); E.V. Linder, [hep-th/0410017](#); Y.S. Myung, [hep-th/0412224](#).
- [10] A. Gregori, [hep-th/0207195](#); A. Gregori, [hep-th/0402126](#).
- [11] T. Padmanabhan, Class. Quant. Grav. 19 (2002) L167, [gr-qc/0204020](#); T. Padmanabhan, Phys. Rept. 406 (2005) 49, [gr-qc/0311036](#); T. Padmanabhan, [hep-th/0406060](#); T. Padmanabhan, [astro-ph/0411044](#).
- [12] E.V. Gorbar, I.L. Shapiro, JHEP 0302 (2003) 021, [hep-ph/0210388](#); I.L. Shapiro, [hep-th/0412115](#).
- [13] G.W. Gibbons, S.W. Hawking, Phys. Rev. D 15 (1977) 2738.
- [14] J.P. Uzan, [astro-ph/0409424](#).
- [15] H. Stefancic, Phys. Rev. D 71 (2005) 084024, [astro-ph/0411630](#); S. Nojiri, S.D. Odintsov, S. Tsujikawa, Phys. Rev. D 71 (2005) 063004, [hep-th/0501025](#).
- [16] S. Eidelman *et al.* [Particle Data Group Collaboration], “Review of particle physics,” Phys. Lett. B 592 (2004) 1.

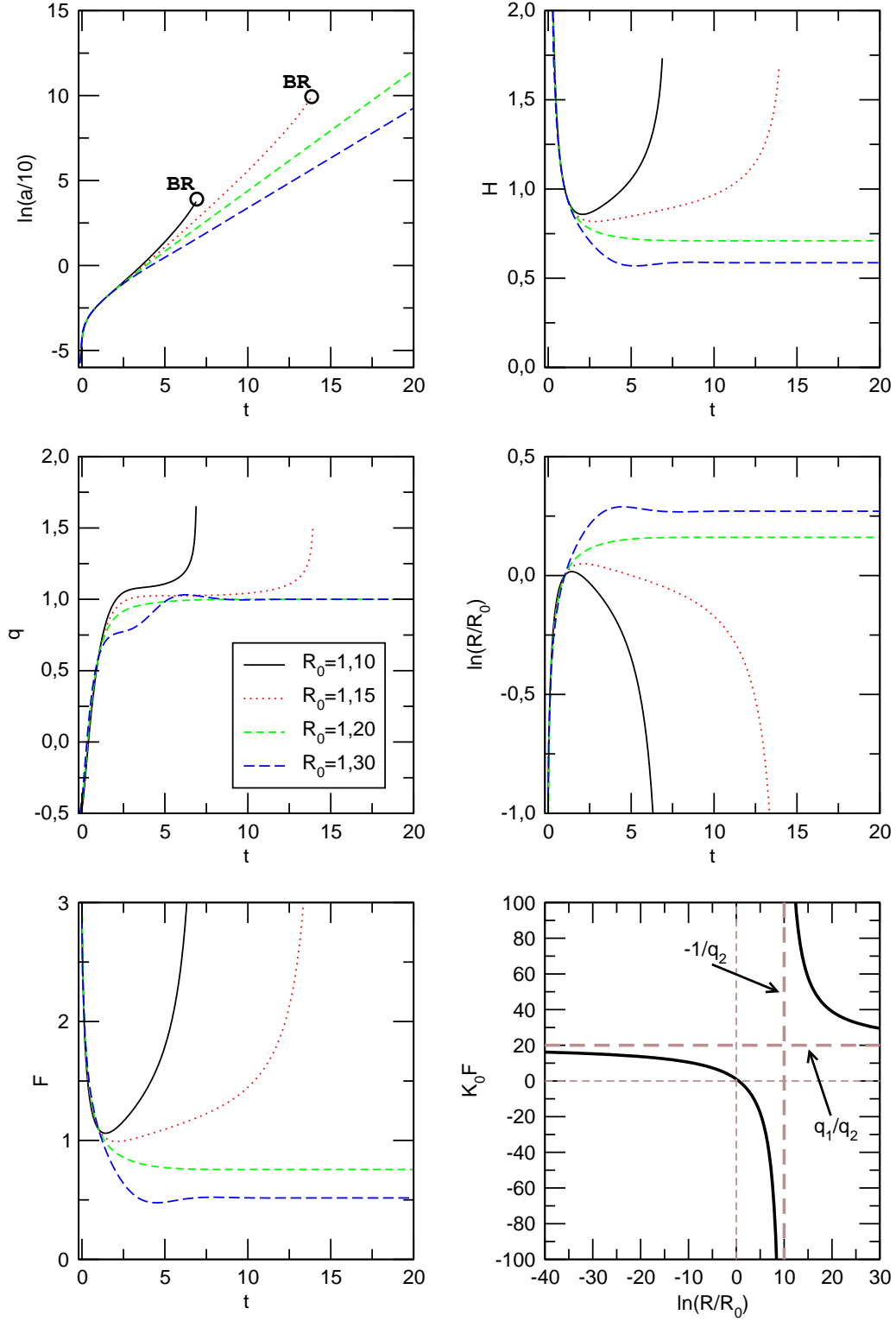


Figure 4: The cosmological evolution for the parameter choice $q_1 = -2$ and $q_2 = -0,1$ and different values of the initial event horizon radius R_0 . The fate of this universe is either a stable de Sitter state when choosing $R_0 = 1,20; 1,30$, or a big rip (BR) in the case $R_0 = 1,10; 1,15$. K_0F is bounded from above. Nomenclature: Scale factor a , Hubble scale $H = \frac{\dot{a}}{a}$, acceleration $q = \frac{\ddot{a}a}{\dot{a}^2}$, event horizon radius R and its initial value R_0 . For the function K_0F see Eqs. (12), (9), and (11), for the mass parameters q_1, q_2 see Eqs. (3) and (5).

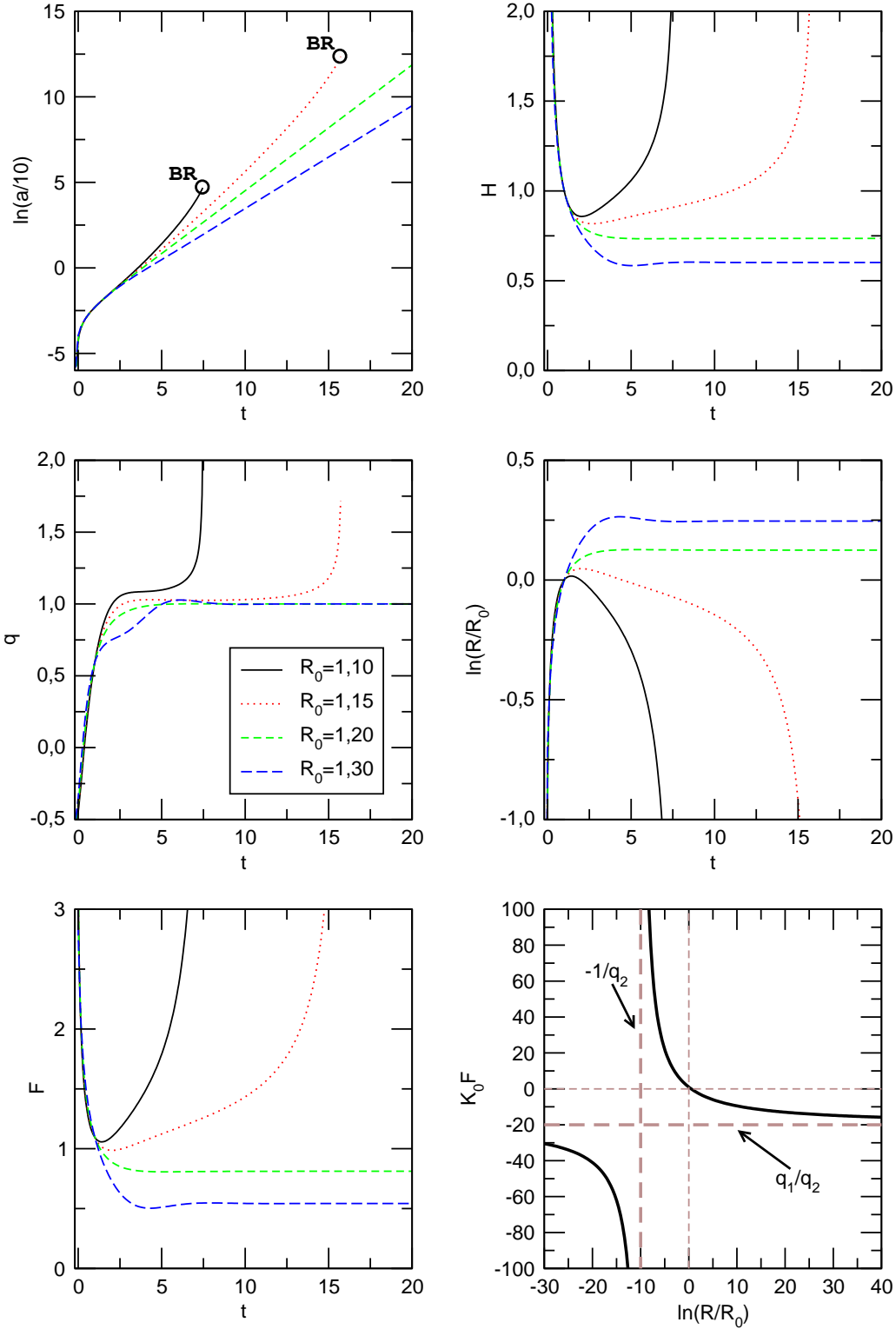


Figure 5: For the parameter choice $q_1 = -2$ and $q_2 = +0,1$ the cosmic evolution is not very different from the case $q_2 = -0,1$ (Fig. 4). In the future, there is either a stable de Sitter state for $R_0 = 1, 20; 1, 30$, or a big rip (BR) when $R_0 = 1, 10; 1, 15$. K_0F is bounded from below. Nomenclature: Scale factor a , Hubble scale $H = \frac{\dot{a}}{a}$, acceleration $q = \frac{\ddot{a}}{a^2}$, event horizon radius R and its initial value R_0 . For the function K_0F see Eqs. (12), (9), and (11), for the mass parameters q_1, q_2 see Eqs. (3) and (5).

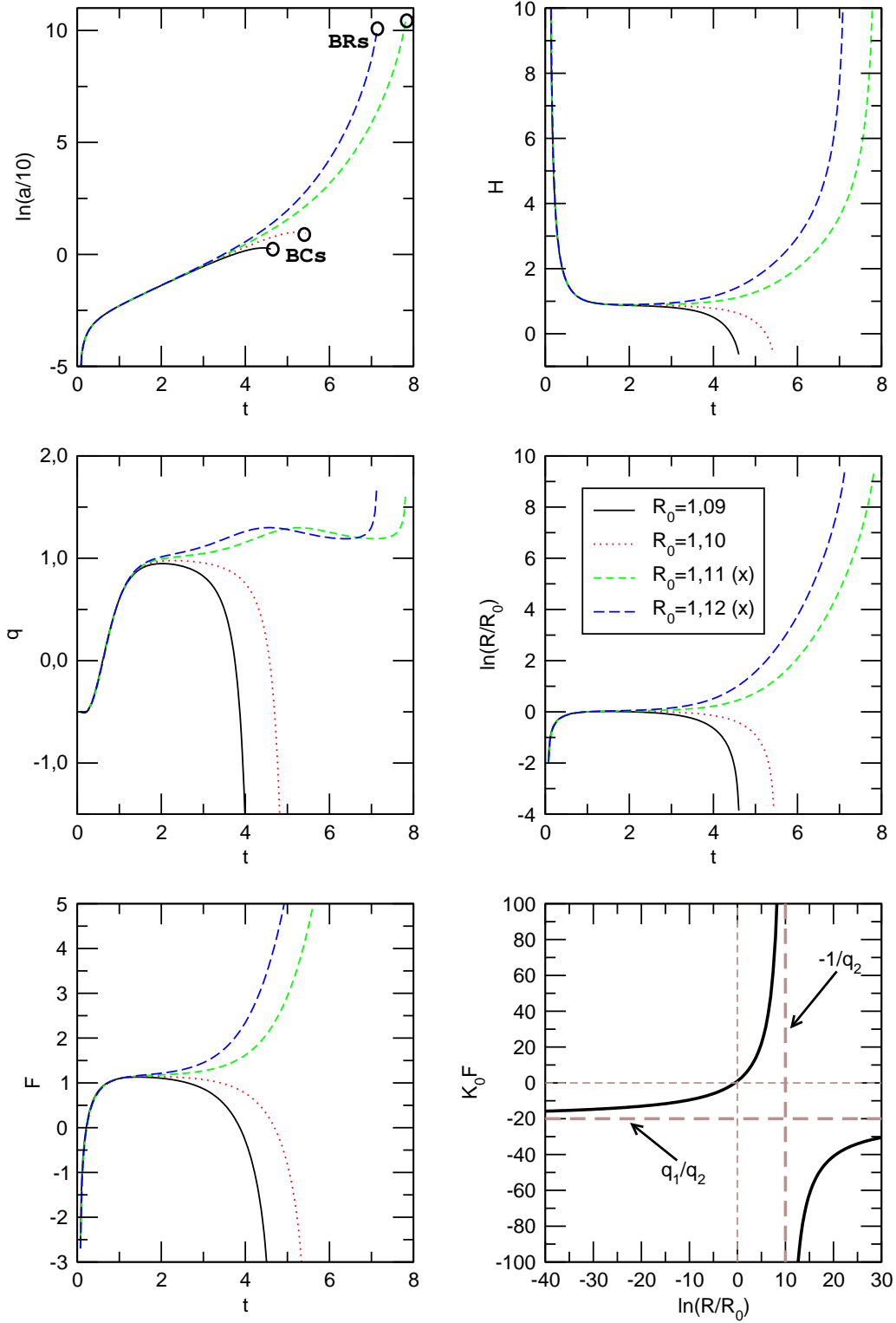


Figure 6: The cosmological evolution for different values of today's horizon radius R_0 for the case $q_1 = +2$ and $q_2 = -0,1$. The solutions for $R_0 = 1,09; 1,10$ exhibit a big crunch (BC), whereas the initial conditions $R_0 = 1,11; 1,10$ lead to a big rip (BR). K_0F is bounded from below. The numerical solutions marked by (x) are not compatible with the main equation (10), see Sec. 5 for further details. Nomenclature: Scale factor a , Hubble scale $H = \frac{\dot{a}}{a}$, acceleration $q = \frac{\ddot{a}}{a^2}$, event horizon radius R and its initial value R_0 . For the function K_0F see Eqs. (12), (9), and (11), for the mass parameters q_1, q_2 see Eqs. (3) and (5).

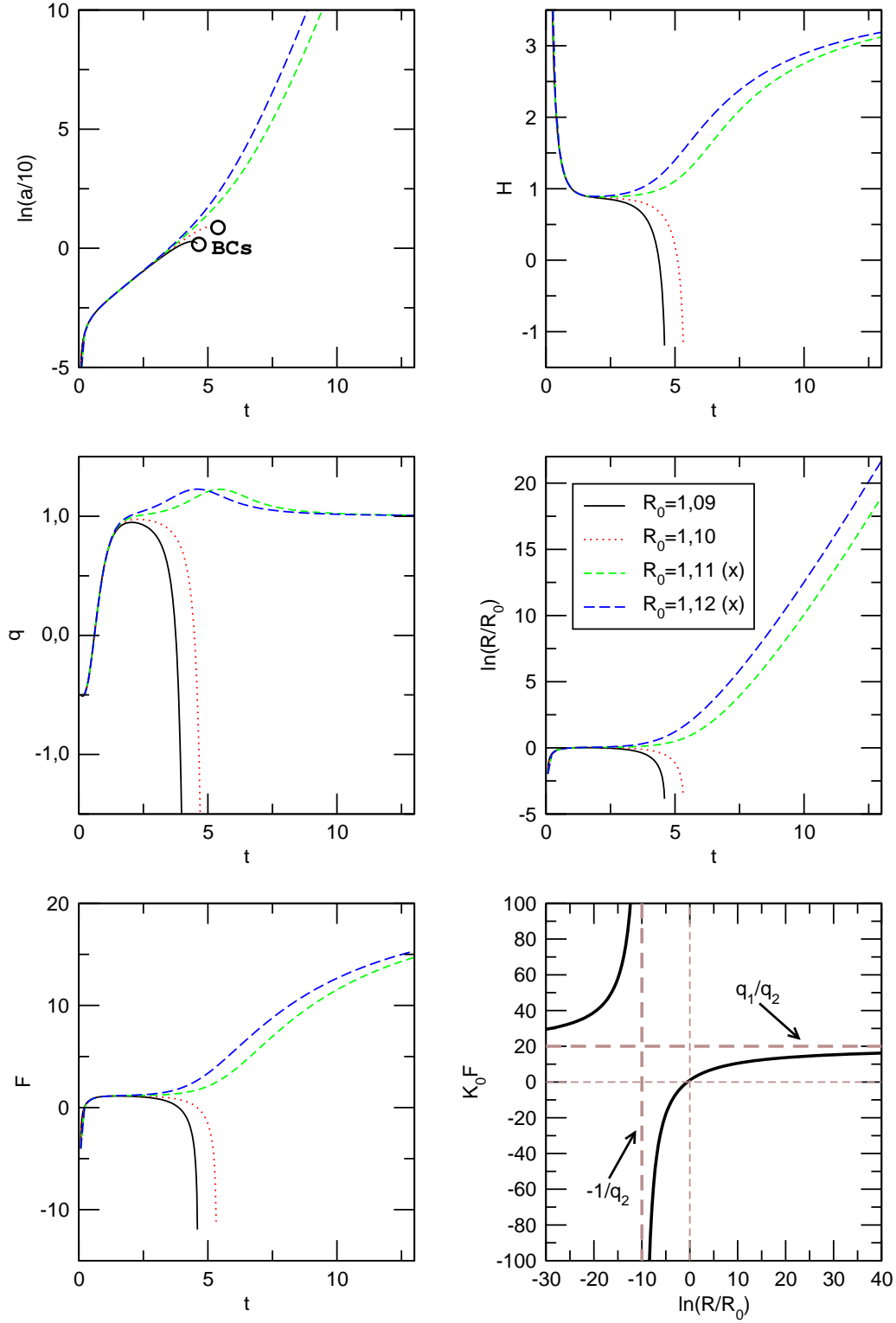


Figure 7: The cosmological evolution for different values of today's horizon radius R_0 . Here, we choose $q_1 = +2$ and $q_2 = +0,1$. The solutions for $R_0 = 1,09; 1,10$ exhibit a big crunch (BC), where K_0F is unbounded from below. For the initial conditions $R_0 = 1,11; 1,10$ the function F and the Hubble scale H approach a finite value, where the horizon radius R diverges. The numerical solutions marked by (x) are not compatible with the main equation (10), see Sec. 5 for further details. Nomenclature: Scale factor a , Hubble scale $H = \frac{\dot{a}}{a}$, acceleration $q = \frac{\ddot{a}}{a^2}$, event horizon radius R and its initial value R_0 . For the function K_0F see Eqs. (12), (9), and (11), for the mass parameters q_1, q_2 see Eqs. (3) and (5).